

# SYNTHESIS AND CHARACTERIZATION OF $Mn_{0.3}Zn_{0.7}Fe_2O_4$ FERRITE WITH SOL-GEL COMBUSTION METHOD

## SINTEZA IN KARAKTERIZACIJA $Mn_{0.3}Zn_{0.7}Fe_2O_4$ FERITA, IZDELANEGA S SOL-GEL ZGOREVALNO METODO

Jing Zhang\*

Wuxi Vocational Institute of Arts & Technology, Yixing 214209, China

Prejem rokopisa – received: 2019-09-20; sprejem za objavo – accepted for publication: 2020-05-02

doi:10.17222/mit.2019.225

Ferrite powders  $Mn_{0.3}Zn_{0.7}Fe_2O_4$  were synthesized with the sol-gel combustion method using manganese nitrate, zinc nitrate, ferric nitrate and citric acid as raw materials. The formation process, structure, surface morphology and electromagnetic performance of samples were characterized using TG-DSC, XRD, SEM and a network analyzer. A spinel ferrite with a pure phase composition and a uniform size distribution of 30–50 nm was prepared in the best preparation conditions including a firing temperature of 1050 °C, holding time of 3 h, ratio of citric acid to nitrate (MRCM) of 1:1 and pH value of 7. The products prepared under these conditions show excellent microwave electromagnetic properties; the reflection loss (RL) of  $Mn_{0.3}Zn_{0.7}Fe_2O_4$  reaches the maximum value of -17.02 dB at 14.1 GHz, but the RL is 10 dB higher in the range of 12.5–15 GHz.

Keywords: Mn-Zn ferrite, sol-gel combustion method, microwave electromagnetic properties

Avtorji tega članka so feritne prahove  $Mn_{0.3}Zn_{0.7}Fe_2O_4$  sintetizirali s sol-gel zgorevalno metodo in zanje kot osnovne surovine uporabili manganov, cinkov in železov nitrat ter citrsko kislino. Proces nastajanja ferita, nanostrukture, površinske morfologije in elektromagnetne lastnosti vzorcev so okarakterizirali s TG-DSC, XRD, SEM in mrežnim analizatorjem. Pripravili so špinelni ferit s čisto fazno sestavo in enovito velikostno porazdelitvijo kristalnih zrn v območju velikosti zrn med 30 nm in 50 nm. Najboljši pogoji izdelave so bili: temperatura žganja 1050 °C, čas zadrževanja na tej temperaturi 3 ure, razmerje med citrsko kislino in nitrati (MRCM) 1:1 ter pH vrednost 7. Ferit  $Mn_{0.3}Zn_{0.7}Fe_2O_4$ , izdelan pod temi pogoji, je imel odlične mikrovalovne elektromagnetne lastnosti in izgube odboja (RL) so dosegle maksimalne vrednosti -17,02 dB pri 14,1 GHz pri tem ferit ni imel RL več kot -10 dB v področju med 12,5 GHz in 15 GHz.

Keywords: Mn-Zn ferit, sol-gel zgorevalna metoda, mikrovalovne elektromagnetne lastnosti

## 1 INTRODUCTION

Due to their crystal structures, ferrite materials fall into three types: spinel type, magnetite type and garnet type.<sup>1-3</sup> At present, spinel and magnetite ferrites are widely used as electromagnetic wave-absorbing materials.<sup>4</sup> Spinel ferrites are utilized as excellent absorbents due to their ferromagnetism and dielectric properties. When an electromagnetic wave passes through, a spinel ferrite can produce both a magnetic loss and a dielectric loss.<sup>5</sup> Because of the unique physical and chemical effects of nanomaterials, nano-spinel ferrites have many excellent properties, such as low saturation magnetic moment, high susceptibility, high coercivity and so on.<sup>6-8</sup> They can also be used for high and ultra-high frequencies.<sup>9</sup> Therefore, nano-spinel ferrites are widely used and their preparation methods are various.<sup>10,11</sup>

Z. J. Ma<sup>12</sup> and other authors prepared a nano-nickel zinc ferrite doped with different amounts of  $Co^{2+}$  using the hydrothermal method; their results showed that the grain-type structure changed from a spherical structure to an irregular quadrilateral structure with the average particle size increased from 35 nm to 60 nm, and the lat-

tice constant increased from 0.8352 nm to 0.8404 nm with the  $Co^{2+}$  doping. A. N. Hapishah<sup>13</sup> and other authors prepared Co-Zn ferrite  $Co_{0.5}Zn_{0.5}Fe_2O_4$  using high-energy ball milling where the highest reflection loss of the sample was -24.5 dB at a frequency of 8.6 GHz. Compared with these methods, the sol-gel method has several advantages, such as low synthesis temperature, good chemical homogeneity, high purity, small particle size, uniform distribution of impurities, etc.<sup>14,15</sup> However, there are few papers on the preparation of spinel ferrites with the sol-gel method. In this paper, Mn-Zn ferrites were prepared using the sol-gel combustion synthesis, and the influence of the calcining temperature, dwell time, ratio of citrate/nitrate (MRCM) and pH value on the phase composition, particle pattern and microwave electromagnetic performance of MnZn ferrites were systematically investigated.

## 2 EXPERIMENTAL PART

### 2.1 Synthesis of the $Mn_{0.3}Zn_{0.7}Fe_2O_4$ powder

Spinel ferrite  $Mn_{0.3}Zn_{0.7}Fe_2O_4$  was prepared with the sol-gel/combustion method using manganese nitrate, zinc nitrate and iron nitrate as the main raw materials, citric acid as the completing agent and combustion assis-

\*Corresponding author's e-mail:  
zhangjing\_20062007@126.com (Zhang Jing)

tance. An analytical pure nitrate solution was weighed according to each stoichiometric ratio, and demonized water was used to make a uniform mixed solution. An appropriate amount of citric acid was added to the above-mentioned hybrid solution and a certain amount of ammonia water was dripped into the mixed solution to adjust the pH value. The beaker containing the solution was placed in a water bath and heated and stirred at a constant temperature of the water bath of 80 °C to form a transparent sticky gel. After that, the wet gel was placed in an electric heating dryer and heated at 180 °C. After several minutes, the gel combusted and a fluffy precursor powder was obtained after the reaction was completed. Finally, the precursor powders were calcined in a definite temperature range, then removed and ground to obtain the required ferrite powders.

## 2.2 Characterization

The precursors for the sol-gel/combustion synthesis were analyzed using TG-DSC with an STA-449C comprehensive thermal analyzer produced by Netzsch. The phase composition of the ferrite was analyzed with RigakuD/Max-2500. The morphology was observed with a scanning electron microscope (Model JSM-5610LV) from the JEOL Company. The electromagnetic parameters of the samples,  $\epsilon'$ ,  $\epsilon''$ ,  $\mu'$  and  $\mu''$ , were measured with an Agilent 8722ET network analyzer in a range of 2–18 GHz, and the electromagnetic losses were calculated. The reflection loss (RL) of the absorber was calculated using the YRComputer software.

## 3 RESULTS AND DISCUSSION

### 3.1 TG-DSC characterization of the precursor

Thermal-analysis results of the  $Mn_{0.3}Zn_{0.7}Fe_2O_4$  precursors are shown in **Figure 1**. The exothermic peak near 352.1° indicates that the decomposition of the gel takes place one step at a time. It can be assumed that the DSC curve of xerogel corresponds to the autocatalytic anionic redox reaction between the nitrate and citrate system. From the thermogravimetric curves of xerogels, the first

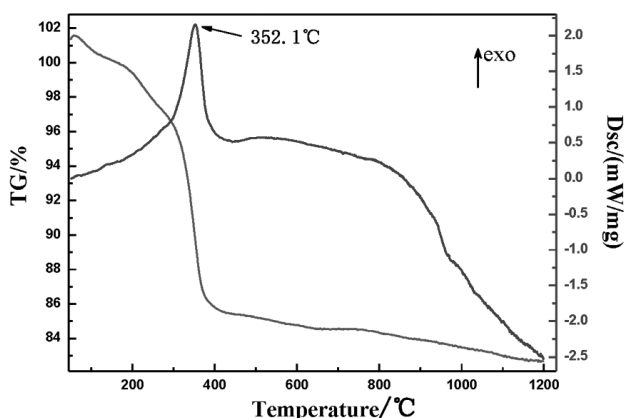


**Figure 1:** TG/DSC curves of  $Mn_{0.3}Zn_{0.7}Fe_2O_4$  precursor

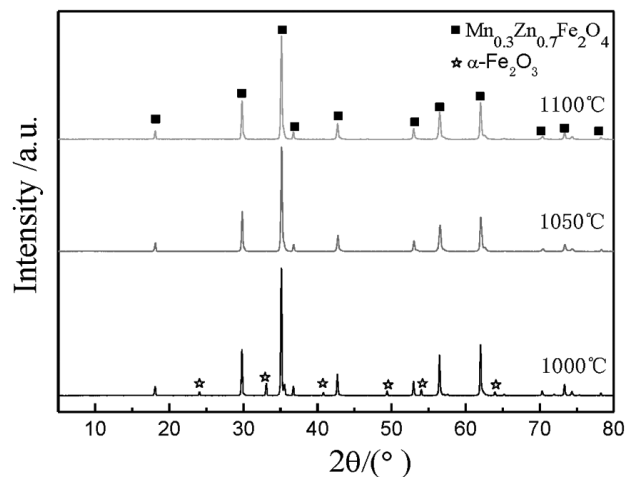


**Figure 2:** XRD patterns of Mn-Zn ferrites calcined at different temperatures

weightlessness (16.8 %) corresponds to the exothermic peak (352.1 °C) in the DSC curve, indicating the removal of citric acid and nitrate. The second small weightlessness (2.1 %) occurs between 500 °C and 1100 °C. When the temperature is higher than 1100 °C, no obvious weightlessness occurs, indicating that the precursor forms a stable phase when the temperature is higher than 1100 °C. Therefore, when the heating rate is determined, it should be relatively slow near 350 °C in order to facilitate a full decomposition of the organic matter.

### 3.2 Calcination temperature

**Figure 2** shows the XRD spectra of the spinel  $Mn_{0.3}Zn_{0.7}Fe_2O_4$  samples prepared by holding them for 3 hours at different calcination temperatures. As shown, the main phase of the powder obtained with the calcination at 1000 °C is spinel ferrite, with a small amount of  $\alpha$ - $Fe_2O_3$  impurities. With an increase in the calcination temperature, the impurity phase of  $\alpha$ - $Fe_2O_3$  disappears gradually. When the calcination temperature is 1050 °C, the synthesized ferrite is a single phase of manganese-zinc ferrite. When the calcination temperature rises to 1100 °C, the structure of the synthesized ferrite samples does not change significantly. Therefore, the final choice of the calcination temperature is 1050 °C.

### 3.3 Calcination time

The crystal structure of spinel ferrite can be characterized with an XRD analysis. **Figure 3** shows the XRD spectra of the Mn-Zn ferrite samples prepared using calcination at 1050 °C for different times. When the calcination time is 1 h, there are still a few impurities beside the manganese-zinc ferrite phase formed. When the calcination time is 3 h, a pure spinel Mn-Zn ferrite phase is formed, with an increase in the characteristic peak strength and a gradual disappearing of the impurity

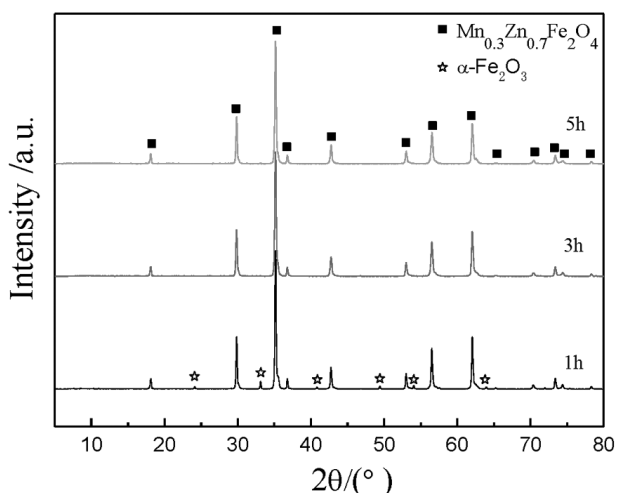


**Figure 3:** XRD patterns of Mn-Zn ferrites calcined at 1050 °C for different times

phase. The phase composition of the samples remains unchanged when the time is extended to 5 h.

SEM was used to identify the morphology and distribution of the products. SEM photographs of spinel ferrite samples calcined at 1050 °C for different times are shown in **Figure 4**. It can be observed that the particle size increases gradually with the increase in the calcination time. After the calcination, particles exhibit irregular granular shapes, the particle distribution across the samples is more uniform and there is slight agglomeration. When the calcination time increases to 5 h, there is slight sintering between the powder particles. Thus, the optimum calcination time is 3 h.

### 3.4 Effect of a citric acid addition

Citric acid plays a dual role in the completing agent and fuel in the sol-gel/combustion synthesis process. The effect of the citric-acid dosage on the state of the precursors and calcined powders is given in **Table 1**. As shown, when the amount of citric acid is insufficient, the metal ions cannot be fully completed to form gels. When the *MRCM* is 1, the gel can self-burn quickly and smoothly so that we finally get a fluffy precursor powder. This happens because there are enough oxidants and reductants in the system. In the heating process, the heat

generated by the redox reaction greatly promotes the diffusion of reactants, which is conducive to the reaction. When citric acid is excessive, citric acid and metal ions form a multi-nucleated ring-structure complex, which improves the stability. It is therefore difficult to oxidize and reduce between citric acid and nitrate, and self-combustion is difficult. The combustion products obtained are dry and non-fluffy.

**Table 1:** Precursor and powder states for different *MRCMs*

Ratio of citric acid to nitrate ( <i>MRCM</i> )	0.5	1.0	2.0
Precursor state	No gel appeared	Gelation is obvious and the precursor is fluffy	Precursor is dry and rigid, not fluffy
Average grain size/nm	41	33	53

In addition, the average grain size of the precursors obtained by calculating different ratios with Jade 5 software and calcining them at 1050 °C for 3 h is listed in **Table 1**. It can be seen that when the *MRCM* is 1, the average grain size is the smallest, which is 33 nm. With an increase in the citric-acid content, the heat release increases and the average grain size grows slightly during the calcination process.

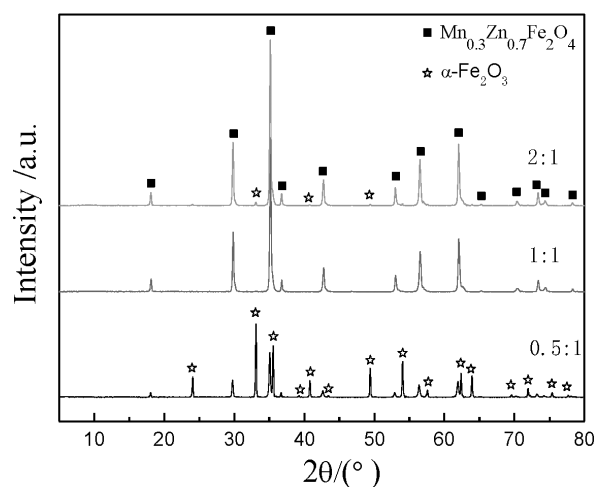


**Figure 5:** XRD patterns of Mn-Zn ferrites under different *MRCM* values

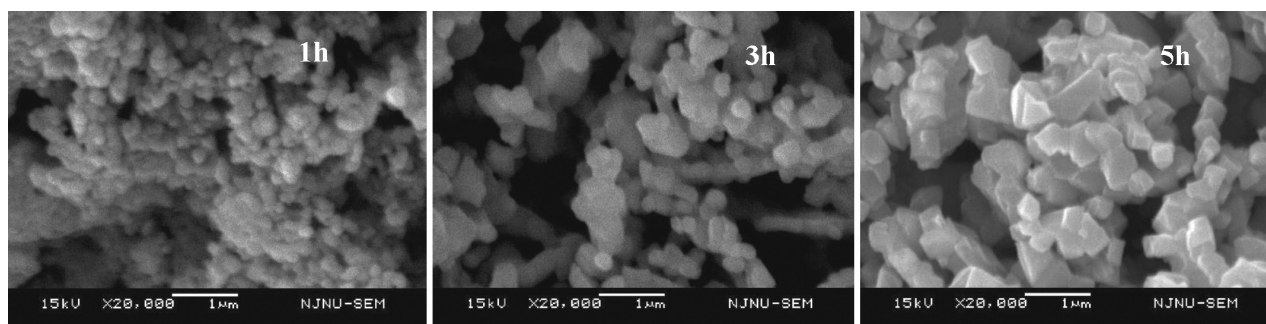


**Figure 4:** SEM photographs of Mn-Zn ferrites calcined at 1050 °C for different times

**Figure 5** shows the XRD spectra of the Mn-Zn ferrite samples prepared with calcination at 1050 °C for 3h with different *MRCMs*. According to **Figure 5**, when the *MRCM* is 0.5, the main phase of the products is α-Fe<sub>2</sub>O<sub>3</sub>, the crystalline phase of Mn-Zn ferrite appears, but the intensity of the diffraction peak is weak. When the *MRCM* is 1, a pure Mn-Zn ferrite crystalline phase is formed, with strong and sharp X-ray diffraction peaks and there are no other impurity peaks. When the *MRCM* increases to 2, a small amount of α-Fe<sub>2</sub>O<sub>3</sub> miscellaneous phase appears. Therefore, the best *MRCM* is 1:1.

### 3.5 Effect of the pH value

The pH value of a solution is an important factor affecting the complexation degree of citric acid and metal ions. If the pH value is too low, the ionization of citric acid is inhibited, which affects its complexation with metal ions. If the pH value is too high, metal ions form a hydroxide precipitation before the complexation of citric acid with metal ions. In order to obtain stable sol-gel, the pH value of the solution should be adjusted so that of the metal ions in the sol system that are completely complexed. **Figure 6** shows the XRD spectra of the Mn-Zn ferrite precursors prepared at different pH values and calcined at 1050 °C for 3 h. When the pH value is 1, there are still a few impurities beside the manganese-zinc ferrite phase; when the pH value is 3, 5, 7, a pure spinel Mn-Zn ferrite phase is formed.

Ferrite is a kind of absorbing material with dual loss characteristics of the magnetic loss and electrical loss. The magnitude of the electromagnetic wave loss can be expressed with the tangent of the loss angle (tan δ), which includes the tangent of the electric-loss angle (tan δ<sub>e</sub>) and tangent of the magnetic-loss angle (tan δ<sub>m</sub>). Their calculation formula is as follows:

$$\tan \delta = \tan \delta_e + \tan \delta_m = \varepsilon''/\varepsilon' + \mu''/\mu' \quad (1)$$

In the formula, ε' and ε'' are the real and imaginary parts of the relative complex permittivity of the material,

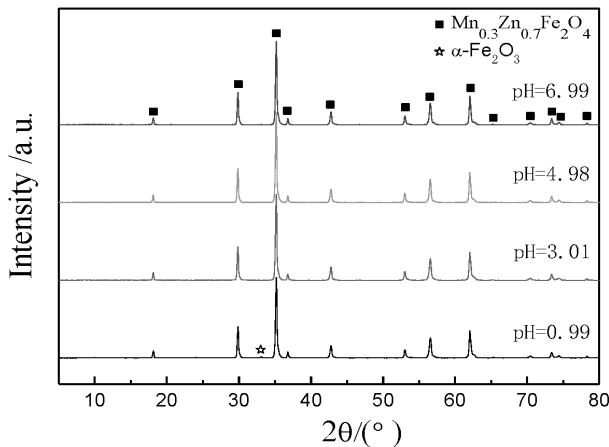


**Figure 6:** XRD patterns of Mn-Zn ferrites prepared at different pH values

and μ' and μ'' are the real and imaginary parts of the relative complex permeability of the material. It can be seen from the formula that the larger the imaginary part of the relative dielectric constant and the imaginary part of the relative permeability of the material, the greater is the absorption loss of the material to the electromagnetic wave and the better is the absorption effect. The magnetic loss is dominant in ferrite, so the imaginary part of permeability should be increased as much as possible.

**Figure 7** illustrates the magnetic loss for the Mn-Zn ferrite precursors prepared at different pH values and calcined at 1050 °C for 3 h in the band of 2–18 GHz. With the change of frequency, the magnetic loss first decreases, then increases, further decreases, shows a mountain-shaped formation, while the value of tan δ reaches the maximum at about 14 GHz. With an increase in the pH value, the value of tan δ shows an increasing trend. When the pH value is 7, it reaches the maximum of 0.47 at the frequency of 14.1 GHz. Thus, the optimum pH value is 7.

### 3.6 Analysis of the microwave-absorbing property

In a single-layer microwave-absorbing coating, the absorbing characteristics can be represented as the reflection loss (RL), described as:

$$RL = 20 \lg \left| \frac{Z_{in} - 1}{Z_{in} + 1} \right| \quad (2)$$

$$Z_{in} = \sqrt{\left( \frac{\mu_r}{\varepsilon_r} \right)} \tanh \left[ j \left( \frac{2\pi f d}{c} \right) \sqrt{(\mu_r \varepsilon_r)} \right] \quad (3)$$

where Z<sub>in</sub> is the incident impedance, ε<sub>r</sub> = ε' - jε'', μ<sub>r</sub> = μ' - jμ'', ε<sub>r</sub> is the complex permittivity, μ<sub>r</sub> is the complex permeability, c and f are the velocity of light and the frequency of microwave in free space, respectively, and d is the thickness of the absorber.

The reflection loss (R<sub>L</sub>) was calculated with the thickness d of the absorber for 2.5 mm. The R<sub>L</sub> curve of Mn<sub>0.3</sub>Zn<sub>0.7</sub>Fe<sub>2</sub>O<sub>4</sub> is shown in **Figure 8**. According to this

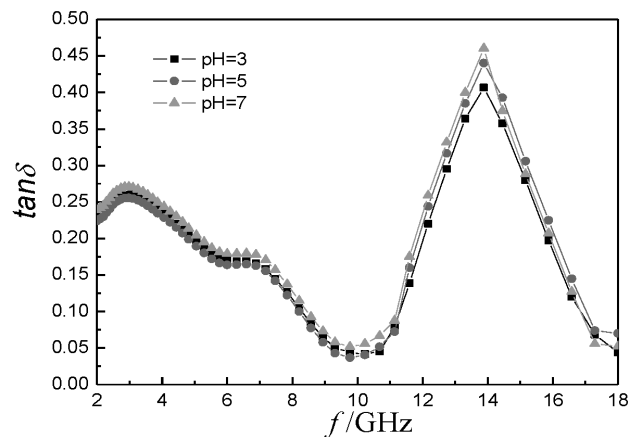


**Figure 7:** Relation between frequency and tan δ of Mn<sub>0.3</sub>Zn<sub>0.7</sub>Fe<sub>2</sub>O<sub>4</sub> prepared at different pH values

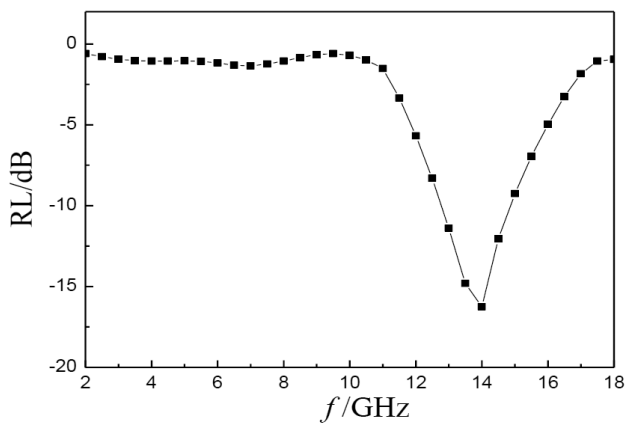


**Figure 8:** Calculated reflection-loss curve for  $\text{Mn}_{0.3}\text{Zn}_{0.7}\text{Fe}_2\text{O}_4$  based single-layer coatings with a matching thickness

figure, the reflection loss reaches the maximum value of  $-17.02$  dB at  $14.1$  GHz, but it is higher by  $10$  dB in the range of  $12.5$ – $15$  GHz. The  $\text{Mn}_{0.3}\text{Zn}_{0.7}\text{Fe}_2\text{O}_4$  ferrite prepared with the sol-gel method shows excellent microwave-absorbing properties.

#### 4 CONCLUSIONS

In this work, Mn-Zn ferrite  $\text{Mn}_{0.3}\text{Zn}_{0.7}\text{Fe}_2\text{O}_4$  was prepared with the sol-gel/combustion synthesis method. The phase composition, particle morphology and microwave-absorbing properties of  $\text{Mn}_{0.3}\text{Zn}_{0.7}\text{Fe}_2\text{O}_4$  were affected by the process parameters. A spinel ferrite with a pure phase composition and uniform size distribution of  $30$ – $50$  nm was prepared in the best conditions including a firing temperature of  $1050$  °C, holding time of  $3$  h, ratio of citric acid to nitrate (MRCM) of  $1:1$  and pH value of  $7$ . Mn-Zn ferrite  $\text{Mn}_{0.3}\text{Zn}_{0.7}\text{Fe}_2\text{O}_4$  prepared with the sol-gel/combustion synthesis method showed good microwave electromagnetic properties; the reflection loss reached its maximum value of  $-17.02$  dB at  $14.1$  GHz, but it became  $10$  dB higher in the range of  $12.5$ – $15$  GHz.

#### 5 REFERENCES

- J. Zhang, L. X. Wang, Q. T. Zhang, Hydrothermal carbonization synthesis of  $\text{BaZn}_2\text{Fe}_{16}\text{O}_{27}$ /carbon composite microwave absorbing materials and its electromagnetic performance, *Journal of Materials Science: Materials in Electronics*, 26 (2015) 4, 2538–2546, doi:10.1007/s10854-015-2720-1
- M. Fu, Z. T. Zhu, Y. J. Zhou, W. Xu, W. Chen, Q. Y. Liu, X. X. Zhu, Multifunctional pompon flower-like nickel ferrites as novel pseudocapacitive electrode materials and advanced absorbing materials, *Ceramics International*, 46 (2020) 1, 850–856, doi:10.1016/j.ceramint.2019.09.042
- J. Zhou, X. F. Shu, Y. Q. Qang, J. L. Ma, Y. Liu, R. W. Shu, L. B. Kong, Enhanced microwave absorption properties of  $(1-x)\text{CoFe}_2\text{O}_4/x\text{CoFe}$  composites at multiple frequency bands, *Journal of Magnetism and Magnetic Materials*, 493 (2020), 165699, doi:10.1016/j.jmmm.2019.165699
- Q. L. Chen, L. Y. Li, Z. L. Wang, Y. C. Ge, C. S. Zhou, J. H. Yi, Synthesis and enhanced microwave absorption performance of  $\text{CIP@SiO}_2@\text{Mn}_{0.6}\text{Zn}_{0.4}\text{Fe}_2\text{O}_4$  ferrite composites, *Journal of Alloys and Compounds*, 779 (2019) 30, 720–727, doi:10.1016/j.jallcom.2018.11.112
- M. Wu, X. S. Qi, R. Xie, Z. C. Bai, S. J. Qin, W. Zhong, C. Y. Deng, Graphene oxide/carbon nanotubes/ $\text{CoFe}_{3-x}\text{O}_4$  ternary nanocomposites: Controllable synthesis and their excellent microwave absorption capabilities, *Journal of Alloys and Compounds*, 813 (2020), 151996, doi:10.1016/j.jallcom.2019.151996
- A. Bahadur, A. Saeed, S. Iqbal, M. Shoaib, I. Ahmad, M. S. Rahman, M. I. Bashir, M. Yaseen, W. Hussain, Morphological and magnetic properties of  $\text{BaFe}_{12}\text{O}_{19}$  nanoferrite: A promising microwave absorbing material, *Ceramics International*, 4 (2017) 9, 7346–7350, doi:10.1016/j.ceramint.2017.03.039
- J. L. Liu, H. S. Liang, Y. Zhang, G. L. Wu, H. J. Wu, Facile synthesis of ellipsoid-like  $\text{MgCo}_2\text{O}_4/\text{Co}_3\text{O}_4$  composites for strong wideband microwave absorption application, *Composites Part B: Engineering*, 176 (2019), 107240, doi:10.1016/j.compositesb.2019.107240
- R. Moučka, N. Kazantseva, I. Sapurina, Electric properties of MnZn ferrite/polyaniline composites: the implication of polyaniline morphology, *Journal of Materials Science*, 53 (2018) 3, 1995–2004, doi:10.1007/s10853-017-1620-6
- S. Tokatlidis, G. Kogias, V. T. Zaspalis, Low loss MnZn ferrites for applications in the frequency region of  $1$ – $3$  MHz, *Journal of Magnetism and Magnetic Materials*, 465 (2018) 1, 727–735, doi:10.1016/j.jmmm.2018.06.056
- K. V. Zipare, S. S. Bandgar, G. S. Shahane, Effect of Dy-substitution on structural and magnetic properties of MnZn ferrite nanoparticles, *Journal of Rare Earths*, 36 (2018) 1, 86–94, doi:10.1016/j.jre.2017.06.011
- M. Rahimi-Nasrabadi, M. Behpour, A. Sobhani-Nasab, M. Rangraz-Jeddy, Nanocrystalline Ce-doped copper ferrite: synthesis, characterization, and its photocatalyst application, *Journal of Materials Science: Materials in Electronics*, 27 (2016) 11, 11691–11697, doi:10.1007/s10854-016-5305-8
- Z. J. Ma, C. Y. Mang, X. Y. Weng, Q. Zhang, L. W. Si, H. T. Zhao, The influence of different metal ions on the absorption properties of nano-nickel zinc ferrite, *Materials*, 11 (2018) 4, 590, doi:10.3390/ma11040590
- A. N. Hapishah, M. M. Syazwan, M. N. Hamidon, Synthesis and characterization of magnetic and microwave absorbing properties in polycrystalline cobalt zinc ferrite  $\text{Co}_{0.5}\text{Zn}_{0.5}\text{Fe}_2\text{O}_4$  composite, *Journal of Materials Science: Materials in Electronics*, 29 (2018) 24, 20573–20579, doi:10.1007/s10854-018-0192-9
- X. R. Zhu, Z. G. Zhu, C. Chen, H. L. Shen, Structural, infrared and magnetic properties of nanosized  $\text{Ni}_x\text{Zn}_{1-x}\text{Fe}_2\text{O}_4$  powders synthesized by sol-gel technique, *Journal of Nanoscience and Nanotechnology*, 15 (2015) 4, 3182–3186, doi:10.1166/jnn.2015.9628
- I. Sadiq, S. Naseem, S. Riaz, S. S. Hussain, M. N. Ashiq, M. Rana, Preparation and characterization of doubly substituted microwave absorbing material by sol-gel technique for super high frequency applications, *Progress in Natural Science: Materials International*, 28 (2018) 4, 478–482, doi:10.1016/j.pnsc.2017.11.001